

NASA TECHNICAL NOTE

TECH LIBRARY KAFB, NM



0069489



NASA TN D-4132

C. I

LOAN COPY: RETURN TO
AFWL (WLJL-2)
KIRTLAND AFB, N MEX

NASA TN D-4132

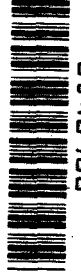
AN EXPERIMENTAL INVESTIGATION OF
THE FREQUENCY AND VISCOSUS DAMPING
OF LIQUIDS DURING WEIGHTLESSNESS

by Jack A. Salzman, Thomas L. Labus, and William J. Mays

Lewis Research Center
Cleveland, Ohio



NATIONAL AERONAUTICS AND SPACE ADMINISTRATION • WASHINGTON, D. C. • AUGUST 1967

TECH LIBRARY KAFB, NM

0069489

AN EXPERIMENTAL INVESTIGATION OF THE FREQUENCY
AND VISCOS DAMPING OF LIQUIDS
DURING WEIGHTLESSNESS

By Jack A. Salzman, Thomas L. Labus, and William J. Masica

Lewis Research Center
Cleveland, Ohio

NATIONAL AERONAUTICS AND SPACE ADMINISTRATION

For sale by the Clearinghouse for Federal Scientific and Technical Information
Springfield, Virginia 22151 - CFSTI price \$3.00

AN EXPERIMENTAL INVESTIGATION OF THE FREQUENCY AND VISCOUS DAMPING OF LIQUIDS DURING WEIGHTLESSNESS

by Jack A. Salzman, Thomas L. Labus, and William J. Masica

Lewis Research Center

SUMMARY

As a part of the general study of liquid behavior in weightlessness, an experimental drop-tower investigation was conducted to determine liquid sloshing characteristics in a zero Bond number environment. The frequency and damping of the fundamental asymmetric sloshing mode in right-circular cylinders (radii ranging from 0.159 to 1.27 cm) were correlated in terms of known system parameters. Contact angles were restricted to very near zero degrees such that the sloshing equilibrium interface was highly curved. Liquid depths were greater than 1 diameter from the cylinder bottom.

INTRODUCTION

A knowledge of the dynamic behavior of liquid propellants in space vehicles has long been of fundamental importance to their control and stability. Recently, the reality of long-range space flights in a weightless or zero gravity environment has created new problems in propellant management. In zero gravity, or, more properly, in a low Bond number environment (Bond number indicates the relative effects of gravity to capillary forces), positioning of the liquid for venting and restart operations becomes of major concern. Investigations establishing the static configuration of the liquid-vapor interface in low Bond number environments have been conducted and the results have been documented (e.g., refs. 1 and 2). Actual space mission requirements, however, include numerous disturbances which may displace the liquid-vapor interface from its static-equilibrium position and induce liquid sloshing. If the frequency of the excitation disturbance is near the natural frequency of the liquid-vapor interface and especially if the damping is small, the slosh amplitude may become large, creating problems in vehicle

control, liquid level sensing, venting, and restart operations. Hence, the frequency and damping associated with the fundamental mode of liquid sloshing in low Bond number environments become basic factors in the propellant management problem.

Investigations of the natural frequency of the liquid-vapor interface in cylinders under various system conditions (i. e., Bond number, contact angle, liquid depth, etc.) are presented in references 3 and 4. For the limiting case of a reasonably flat interface, the theories agree quite well with experimental data. However, as the contact angle and Bond number approach zero, such that the interface is highly curved, the solutions require numerical approximations. For highly curved interfaces, only limited experimental data are available for comparison with the analytic approximations.

Examples of analytic studies concerned with the viscous damping of oscillatory liquid motion may be found in references 5 to 7. The results of experimental 1-g damping investigations (refs. 6 to 9) verify the essentials of viscous damping theory except that the empirical magnitude of the damping observed was slightly higher than that predicted. Damping investigations of a highly curved interface appear to be nonexistent.

The purpose of this report is to present the results of an experimental investigation conducted at the NASA Lewis Research Center on liquid sloshing phenomena in cylindrical containers under effectively zero Bond number conditions. Contact angles were restricted to very near zero degrees such that the liquid-vapor interface was highly curved. Liquid depth was greater than one diameter from the cylinder bottom. The data obtained on natural frequency and damping characteristics are presented and correlated in terms of known system parameters. Also presented are observations of the liquid behavior during slosh including the effects of contact angle variation and large initial amplitudes.

SYMBOLS

A_0	initial slosh amplitude, cm
A_n	n^{th} cycle slosh amplitude, cm
a	system acceleration, cm/sec^2
Bo	Bond number, $Bo = aR^2/\beta$
g	acceleration due to gravity, cm/sec^2
K_0, K_1, K_1', K_2	nondimensional constants
L	interface height above cylinder bottom, cm
n	cycle number
R	cylinder radius, cm

t	time, sec
t_f	formation time, sec
X_l	instantaneous interface displacement from sloshing equilibrium at cylinder wall, cm
α	damping coefficient, sec^{-1}
β	specific surface tension, σ/ρ , cm^3/sec^2
λ	damping factor, α/ω_0
δ	logarithmic decrement, $\delta = (1/n) \ln (A_n)/(A_{n+1})$
θ	contact angle, deg
μ	viscosity, cP
ν	kinematic viscosity, μ/ρ , cm^2/sec
ρ	density, g/cm^3
σ	surface tension, dynes/cm
Ω^2	natural frequency parameter, $\Omega^2 = (R^3 \omega_0^2 / \beta)$
ω_d	damped system frequency, rad/sec
ω_0	system natural frequency, rad/sec
$\bar{\omega}_0$	average measured frequency, rad/sec

APPARATUS AND PROCEDURE

The experimental investigation was conducted in a 2.3-second drop tower (fig. 1). Aerodynamic drag on the experimental package was kept below 10^{-5} g by allowing the package to fall freely within a protective drag shield. The experiment package which was used to conduct the slosh study is shown in figure 2. An air cylinder was used to apply a lateral disturbance to a low-friction slide. Precision diameter borosilicate glass cylinders, ranging in radii from 0.159 to 1.27 centimeters, were mounted on this slide. An adjustment of the air-cylinder stroke and pressure to obtain the desired initial slosh amplitude was determined experimentally and set prior to each drop. A 16-millimeter high-speed motion picture camera was used to record time and displacement characteristics of the liquid behavior. These films were subsequently analyzed on a motion analyzer which magnified the image eight times and permitted displacement measurements down to 0.02 centimeter. In an attempt to view the liquid-vapor interface more accurately, a backlighting scheme was employed. Basically, this scheme consisted of a tapered section of clear plastic with the side facing the camera vapor-blasted. This

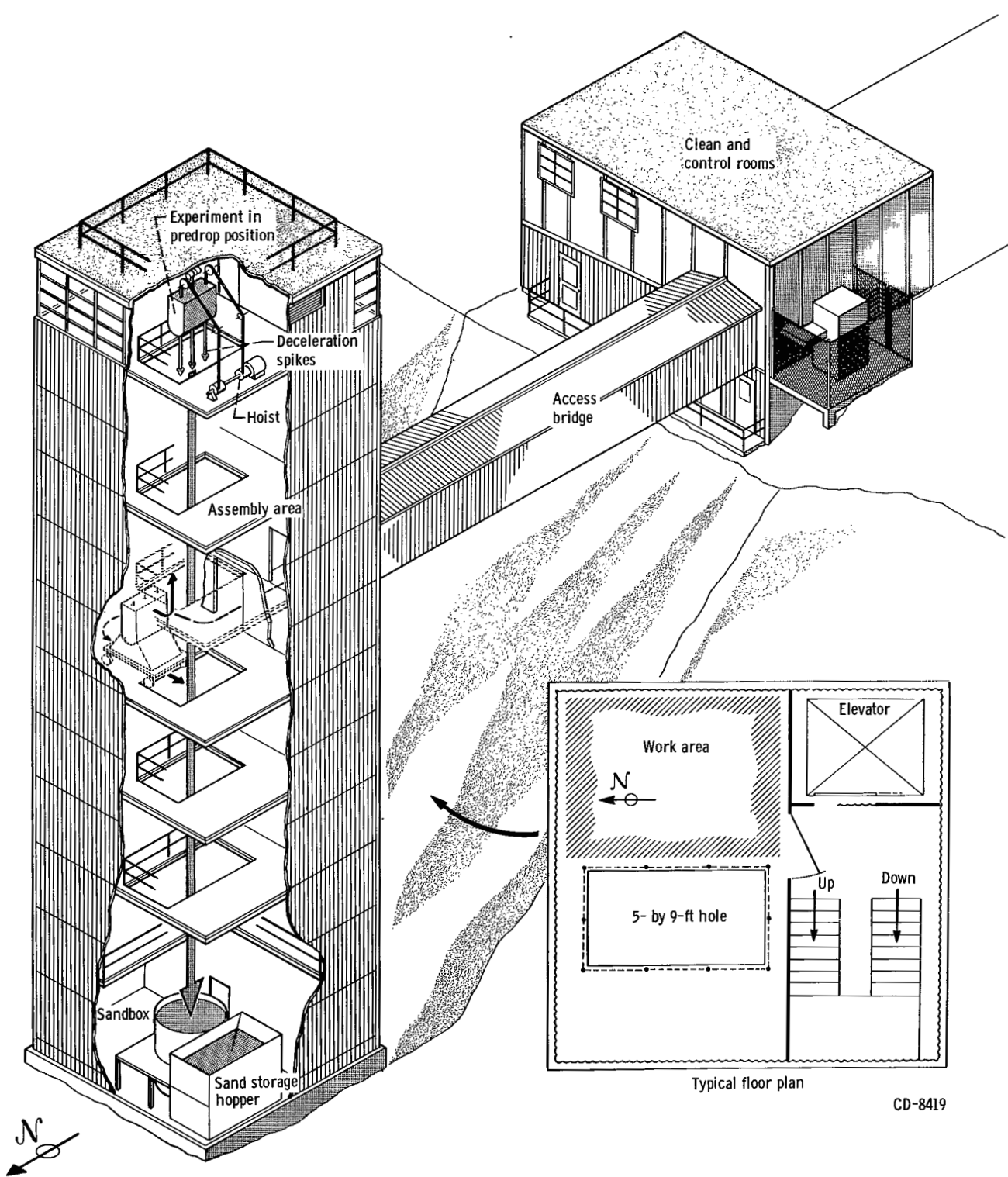


Figure 1. - 2.3-Second drop tower.

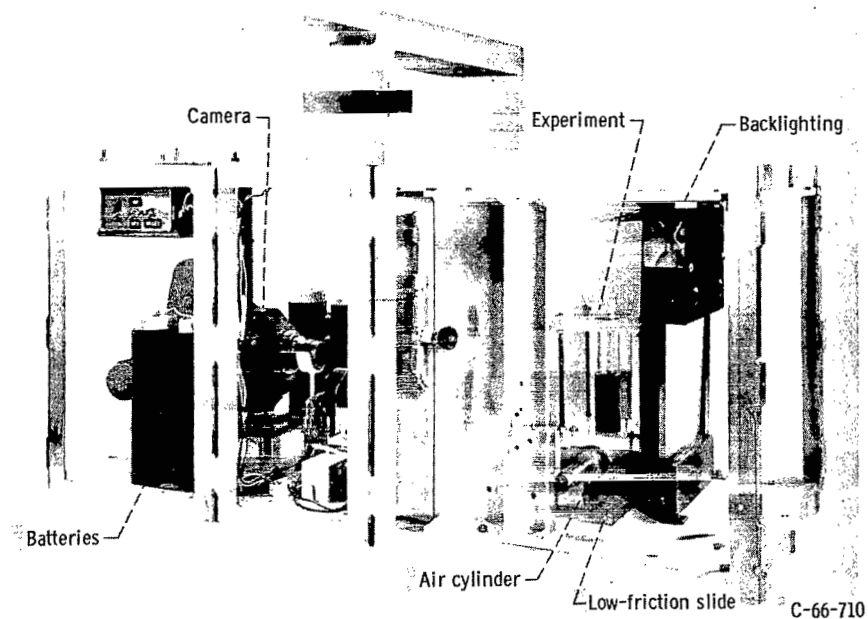


Figure 2. - Experiment package.

method ensured uniform illumination by diffusing the entering light. Time measurements were obtained by viewing a precision digital clock with a calibrated accuracy of 0.01 second.

Analytic reagent grade liquids were used possessing static equilibrium contact angles near zero degrees. The properties of these liquids can be found in table I. Contamination of the glass surfaces and liquids, which could alter the surface tension and contact angle of the test liquid, was carefully avoided. The glassware was cleaned ultrasonically in a detergent solution, rinsed with distilled water and dried in a warm air dryer.

During the test drop, the application of the lateral disturbance was preceded by a predetermined time increment to allow the zero-gravity configuration to form. The minimum time required for the interface to reach a sufficiently quiescent configuration was empirically determined to be

$$t_f = 1.8 \left(\frac{R^3}{\beta} \right)^{1/2} \quad (1)$$

While this allowed formation time was generally not sufficient to ensure a completely quiescent, highly curved interface, the motion was sufficiently damped so that it had no effect on the ensuing slosh wave.

TABLE I. - SUMMARY OF PARAMETERS

Liquid	Surface tension ^a , σ , dynes/cm	Density ^a , ρ , g/cm ³	Liquid viscosity ^a , μ , cP	Cylinder radius, R , cm	Actual measured frequencies, ω_0' , rad/sec	Average frequency, $\bar{\omega}_0$, rad/sec	Logarithmic decrement, δ	Liquid	Surface tension ^a , σ , dynes/cm	Density ^a , ρ , g/cm ³	Liquid viscosity ^a , μ , cP	Cylinder radius, R , cm	Actual measured frequencies, ω_0' , rad/sec	Average frequency, $\bar{\omega}_0$, rad/sec	Logarithmic decrement, δ						
Trichloro-trifluoro-ethane	18.6	1.579	0.7	0.159	88.4	86.7	----	Carbon tetrachloride	26.9	1.595	0.97	0.159	101.0	103.6	----						
					82.8								0.317	36.1							
					77.7								0.317	40.5	39.1	0.93					
					97.7								0.476	20.0							
				0.317	30.2	29.6	0.98						0.476	23.4	21.7	0.99					
					32.3								0.635	11.1							
					26.8								0.635	10.2							
				0.635	10.6	10.6	0.99						0.794	6.8	6.8	----					
					10.6								0.952	5.5							
				0.794	6.8								0.952	5.5							
Anhydrous ethanol	22.3	0.789	1.2	0.317	46.0	50.2	1.60	Acetone	23.7	0.792	0.32	0.317	52.3	51.6	0.70						
					49.9								0.635	51.5							
					54.7								0.635	51.1							
				0.635	16.8	17.4	1.27						0.794	17.6	17.1	0.69					
					17.4								0.952	16.6							
					17.1								0.952	17.8							
					18.4								1.270	6.1	6.1	----					
				0.952	9.9	9.9	1.10						0.952	10.4							
					10.4								1.270	9.4							
					9.4								1.270	6.1							
Methanol	22.6	0.793	0.60	0.317	44.2	46.1	1.21	1-Butanol	24.6	0.809	2.90	0.317	61.5	60.4	2.08						
					48.2								0.635	59.2							
					45.7								0.635	19.0	21.3	2.18					
				0.635	16.1	17.0	0.95						0.794	22.4							
					18.0								0.794	15.3	13.3	1.91					
					16.3								0.952	11.2							
					17.8								0.952	10.8	11.4	1.47					
				0.952	9.4								0.952	9.4							
					9.4								0.952	9.4							
					9.4								0.952	12.1							

^aAt 20° centigrade.

PREVIOUS INVESTIGATIONS

It was assumed that, during the fundamental slosh mode, the instantaneous displacement of the liquid-vapor interface at the cylinder wall X_l can be described by an equation of the form

$$X_l = A_0 e^{-\alpha t} \sin(\omega_d t) \quad (2)$$

The damped system frequency ω_d is related to the natural frequency ω_0 by the relation

$$\omega_d = (\omega_0^2 - \alpha^2)^{1/2} \quad (3)$$

such that, if the damping coefficient α is small,

$$\omega_d \approx \omega_0 \quad (4)$$

For convenience, the damping effect is often described in terms of the logarithmic decrement δ where

$$\delta = \frac{2\pi\alpha}{\omega_d} = \frac{1}{n} \ln \frac{A_n}{A_{n+1}} \quad (5)$$

The correlation of the natural frequency ω_0 and the logarithmic decrement δ in terms of basic system parameters is the subject of this report. The study was concerned specifically with small amplitude asymmetric sloshing about a highly curved interface (i.e., zero Bond number and zero degree contact angle) in a cylindrical container.

Low Bond number sloshing in right-circular cylinders has been investigated in references 3 and 4. These linearized inviscid analyses include the effects of contact angle and interface curvature on the system sloshing frequency. For the special case of a flat equilibrium surface (or a 90° contact angle), the fundamental asymmetric sloshing frequency may be expressed nondimensionally as

$$\Omega^2 = [6.255 + 1.841 Bo] \tanh(1.841 L/R) \quad (6)$$

where the frequency parameter constant Ω^2 is defined as

$$\Omega^2 = \frac{R^3 \omega_0^2}{\beta} \quad (7)$$

For large Bond numbers and liquid-depth ratios, these expressions reduce to the familiar normal-gravity equation

$$\omega_0^2 = 1.841 \text{ g/R} \quad (8)$$

For other contact angles at arbitrary Bond numbers, no simple relation exists and numerical techniques are required for solution. A suggested empirical approximation is given in reference 1 of the form

$$\Omega^2 = [6.255 + 1.841 \text{ Bo} - 4.755 \cos \theta] \tanh 1.841(L/R) \quad (9)$$

For zero Bond numbers, zero degree contact angles and $L/R > 2$ equation (9) reduces to

$$\Omega^2 = 1.5 \quad (10)$$

An extrapolation of the results of Satterlee and Reynolds (ref. 3, in particular, fig. 5) and the limited experimental data applicable to zero degree contact angles (ref. 3, p. 178) indicates a value for equation (10) approximately between 2 and 3.

Normal-gravity, high Bond number, investigations of viscous damping in cylinders may be found in references 6 to 9. These studies consider small amplitude oscillations and implicitly assume 90° contact angles. Their results have shown that viscous dissipation in an assumed laminar boundary layer at the cylinder wall and bottom is the primary cause of damping. For large liquid-depth ratios ($L/R > 2$), the damping is practically a result only of dissipation at the cylinder wall. Its magnitude is described by the relation (ref. 8)

$$\delta = K_0 \nu^{1/2} R^{-3/4} g^{-1/4} \quad (11)$$

or its equivalent form

$$\delta = K_1 \left(\frac{\nu}{\omega_0 R^2} \right)^{1/2} \quad (12)$$

obtained by substituting equation (8) into equation (11). The value of K_1 in equation (12) for high Bond number sloshing has been empirically determined to be about 6.1 (ref. 8). Investigations of the damping in a low Bond number environment appear nonexistent.

RESULTS AND DISCUSSION

Behavior of the Interface During the Fundamental Slosh Mode

A schematic of the liquid-vapor interface profile during the fundamental slosh mode is shown in figure 3. In this study, the height of the lowest point on the interface from the cylinder bottom (L) was maintained greater than $2R$. The instantaneous displacement of the edge of the interface at the cylinder wall from the sloshing equilibrium position is defined by X_l . For small slosh amplitudes ($A_0 \leq 0.5 R$), the vertex of the interface remained stationary with respect to the longitudinal axis of the cylinder. The smooth curvature of the interface is representative of the small amplitude, fundamental slosh mode observed in all test runs.

Figure 4 shows a series of photographs illustrating the interface behavior during a typical test run. The initial amplitude was produced by first accelerating the experiment cylinder laterally (fig. 4(b)) and then providing a quick-stop impulse (fig. 4(c)). Although the interface is distorted by the large impulse caused by the quick stop (figs. 4(b) and (c)), it quickly assumes its well-behaved normal sloshing configuration as can be seen in the subsequent oscillations (figs. 4(d) and (e)).

The motion of X_l along both boundaries was recorded during each test run. A representative set of data showing almost two complete cycles of oscillation is given in figure 5. In general, for small amplitudes, the displacements of the two edges were

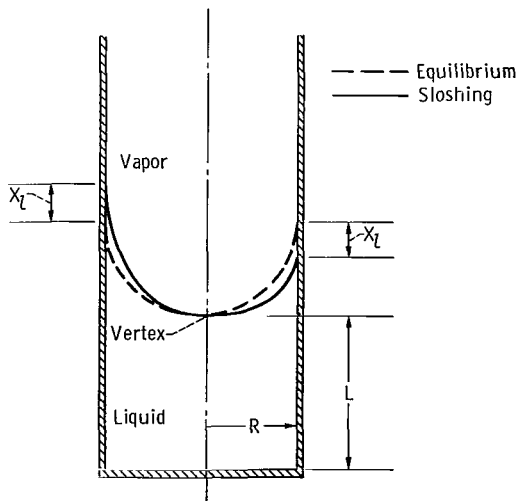
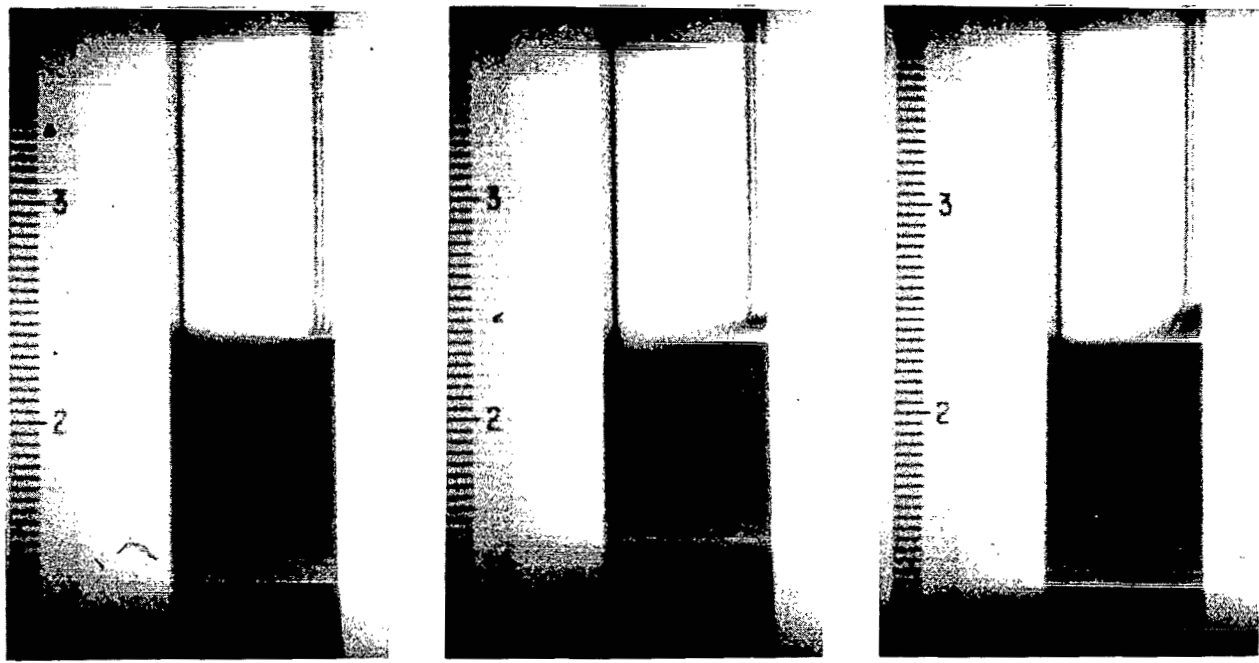


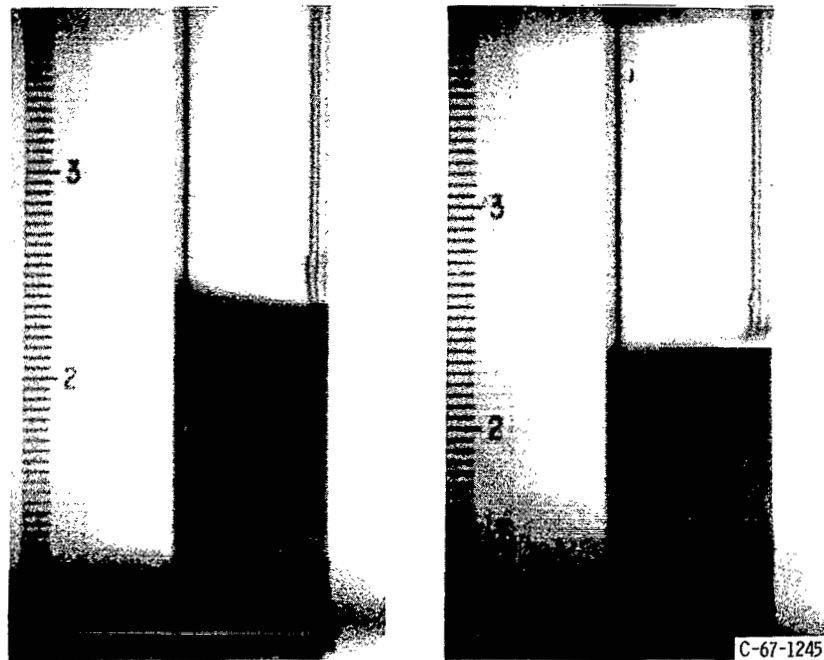
Figure 3. - Interface profile during fundamental slosh mode.



(a) Zero-gravity configuration.

(b) Application of acceleration by air cylinder.

(c) Impulse at end of stroke.



(d) Interface reaches maximum slosh amplitude.

(e) Decayed oscillations continued about sloshing equilibrium.

Figure 4. - Motion of the liquid-vapor interface during a typical data run.

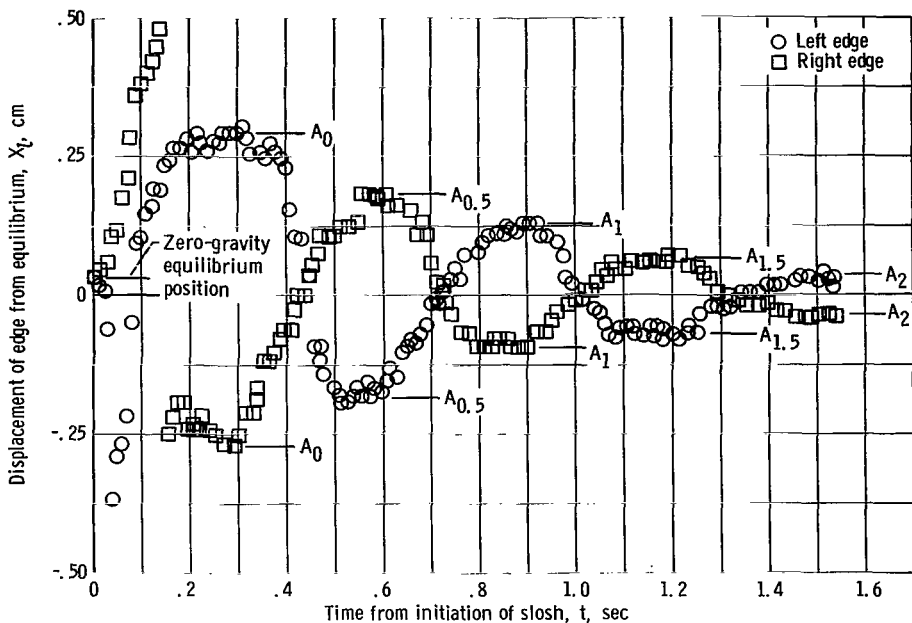


Figure 5. - Interface edge displacement, X_L , during representative data run. Cylinder radius, 0.635 centimeter; specific surface tension, 11.8 centimeters cubed per second squared.

approximately equal and in phase. Although, normally, the position of the interface edge is easily measured, at one point in the test run judgement of the actual edge position is required. When the cylinder motion is abruptly stopped, the right edge of the interface which has been initially displaced upward (fig. 5) continues to advance while the remainder of the interface begins to shift toward the opposite boundary. The initial advancing edge then thins out until only a film of liquid remains. The actual interface edge gradually reappears below the equilibrium position. Thus, there is no sudden drop in the edge position as might be assumed from the initial portion of figure 5, but rather only a lapse in its determination. The residual liquid film left on the cylinder wall caused by the initial amplitude produces a slight drop in the sloshing equilibrium position as compared with the zero Bond number equilibrium configuration (e.g., fig. 5). No additional change in the sloshing equilibrium position was measured during the remaining test time. The liquid film remains on the wall and sloshing actually occurs on a thin layer of liquid rather than on an unwetted surface.

Natural Frequency Results

The half-periods of oscillation in each test run were measured and the corresponding frequency values were calculated using the recorded positions of both interface edges. A tabulation of these frequencies and the subsequent average frequency of each run is

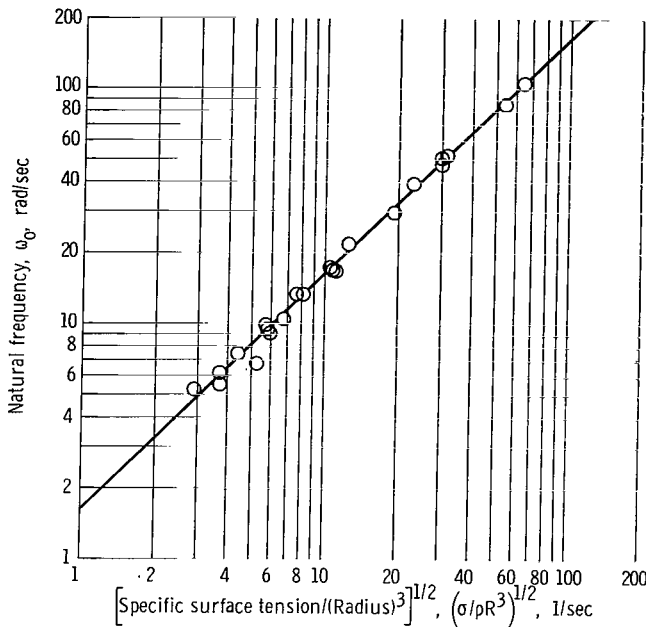


Figure 6. - Experimental correlation of natural frequency. Specific surface tensions, 11.8 to 29.9 centimeters cubed per second squared; cylinder radii, 0.159 to 1.270 centimeters.

listed in table I. The periods of oscillation of any particular system were relatively constant as indicated by the frequencies listed. From these data, the empirical value for Ω^2 in equation (7) was determined to be 2.6 by calculating its value for each measured frequency (i.e., each half period) and then computing a simple arithmetic average. As a measure of uncertainty, the standard deviation of Ω^2 was calculated and determined to be 0.41. A plot of the average frequencies as a function of the ratio $\beta^{1/2}/R^{3/2}$ is shown in figure 6 along with the calculated line representing the equation

$$\omega_0^2 = 2.6 \sigma/\rho R^3 \quad (13)$$

From this figure it can be seen that the experimental data does follow the relation given by equation (13).

It is realized that the measured frequency shown is not truly the natural frequency of the system, but rather a damped frequency. However, the damping coefficient was sufficiently small such that the approximation in equation (4) was valid. Calculations using the measured values of δ showed that the variation was less than 5 percent.

From equation (1) which predicts formation time requirements, and equation (13), which yields the time required for a period of slosh oscillation, it is evident that the limitations on the lower value of β/R^3 and consequently the highest value of R used in this study were imposed by the time restrictions of the test facility (i.e., 2.22 seconds of zero-gravity time). Values of β ranged from 11.8 to 29.9 cubic centimeters per

second squared; R values were varied from 0.159 to 1.270 centimeters.

Contact-angle effects. - All liquids employed in this study exhibited near zero degree static-contact angles on the cylinder surfaces. Since the contact angle will affect the natural frequency (refs. 3 and 4), particular care was taken to avoid inducing finite-contact angles during the slosh motion. As indicated in reference 10, finite-contact angles could be introduced during flow, even though the static angle is zero. While the results of reference 10 are strictly applicable only for steady flow, the effect of viscosity as reported was of equal importance in sloshing motion - the larger the viscosity, the more likely a finite-contact angle. The photograph in figure 7 shows the large contact angle induced for a fluid with a viscosity of 15 centipoise. No measurable contact-angle variations were observed for the data in table I. However, when using butanol (viscosity of 2.9 cP), it was easy to obtain large contact-angle variations. The butanol data were not used in determining Ω^2 because of the possibility of erroneously raising its value.

Viscous Damping Results

Damping of the interface oscillations was determined by observing the decay of the slosh amplitudes A_n of each successive cycle. As an example, the amplitudes recorded in figure 5 are plotted in figure 8. On this semilogarithmic plot, the straight line representation of the data indicates that the damping is exponential. This was representative of all small amplitude test runs. Therefore, the damping magnitude may be measured in terms of the logarithmic decrement defined in equation (5). The magnitude of δ was obtained by hand-fitting a straight line through the points (e.g., fig. 8). The values of δ are tabulated for each data run in table I.

Dimensional analysis of the logarithmic decrement and the pertinent system variables yielded the grouping, $\mu^2/\rho\sigma R$. This grouping together with a parametric analysis of the data yielded the following damping relation

$$\delta = K_2 \left(\frac{\mu^2}{\rho\sigma R} \right)^{1/4} \quad (14)$$

The value of K_2 was calculated from each data point, and its average value was determined to be 21.6 with a standard deviation of 2.2. A plot of equation (14) along with the data is shown in figure 9. Equation (14) may be rewritten in terms of the natural frequency permitting comparison with normal gravity damping by substitution of equation (7) which yields

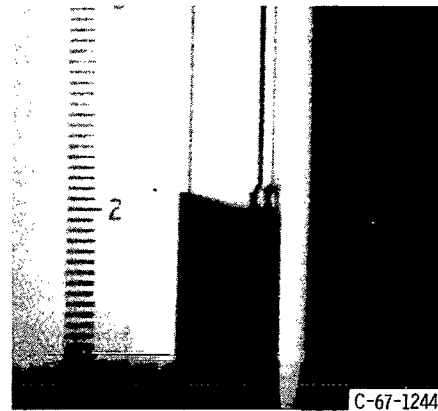


Figure 7. - Contact angle variation during slosh.
Liquid viscosity, 15 centipoise.

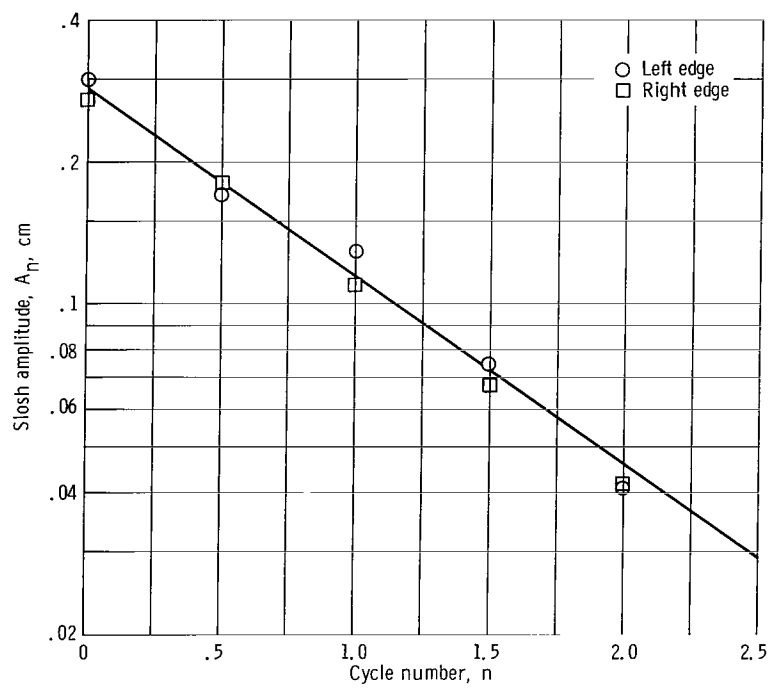


Figure 8. - Damping of interface oscillations during representative data run.

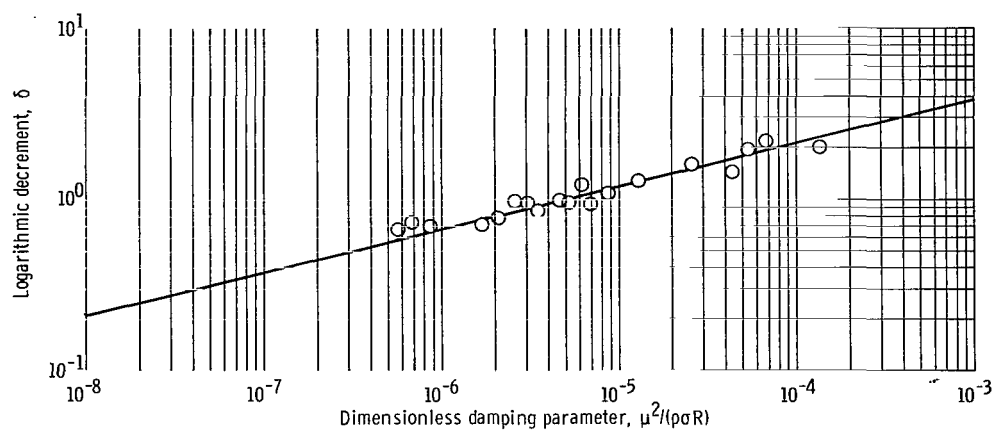


Figure 9. - Zero Bond number damping as a function of system variables.

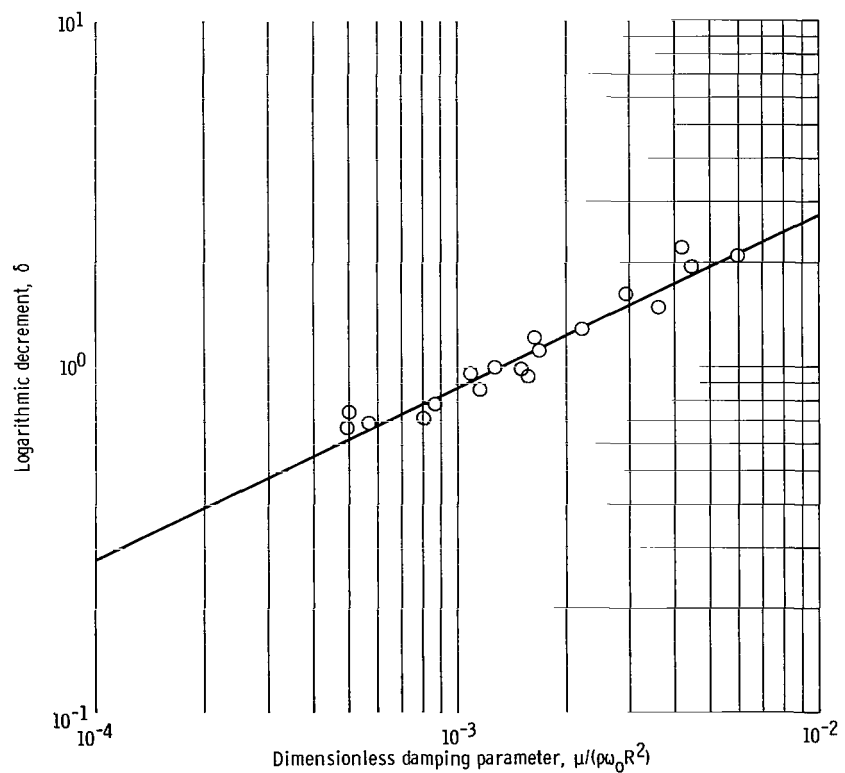


Figure 10. - Zero Bond number damping as a function of system variables and measured frequency.

$$\delta = K'_1 \left(\frac{\mu}{\rho \omega_0 R^2} \right)^{1/2} \quad (15)$$

The forms of equations (12) and (15) are similar; this would tend to indicate that the cause of damping in zero gravity is viscous dissipation in a boundary layer adjacent to the cylinder wall. A plot of equation (15) along with the data appears in figure 10. Using the measured values of ω_0 and δ yielded a value of K'_1 of 28.1 with a standard deviation of 2.5. This value also agrees with the value of K'_1 obtained when the independently determined constants Ω^2 and K_2 are used. Comparing K'_1 and K_1 in equation (12) for high Bond numbers indicates that the constant is about four times greater in a zero Bond number environment.

Amplitude Dependence

The empirical correlations describing the natural frequency and logarithmic decrement are valid for slosh amplitudes less than 0.5 R. In this amplitude range, the natural frequency was observed to be constant for any particular system (i.e., it did not vary with amplitude) and the damping was observed to be exponential. An attempt was made to determine the maximum amplitude to which the frequency and damping correlations remained valid, but no conclusive results were obtained. While it was possible to obtain initial amplitudes as high as 1.0 R, the amplitude after the first half cycle of oscillation always decayed to less than 0.5 R. Since several half periods of oscillation were required for a frequency measurement, the effect of amplitudes in this range on frequency could not be obtained. It is noted, however, that, for amplitudes above 0.5 R, the initial amplitudes were generally not equal and the position of the vertex of the interface was no longer stationary.

SUMMARY OF RESULTS

An experimental investigation was conducted to determine the natural frequency and damping characteristics of the liquid-vapor interface in a zero Bond number (zero-gravity) environment. The study employed flat-bottomed right-circular cylinders and liquids possessing near zero degree contact angles on the cylinder walls. The liquids had viscosities μ between 0.32 and 2.9 centipoise and specific surface tensions β between 11.8 and 30.4 cubic centimeters per second squared. The range of radii R employed was from 0.159 to 1.270 centimeters. Under the stipulation that the liquid-

vapor interface is greater than 2 radii from the tank bottom, that the initial slosh amplitude is less than 0.5 R, and that the contact angle does not vary during sloshing, the investigation yielded the following results:

1. The constant Ω^2 in the natural frequency relation, $\omega_0^2 = \Omega^2 \beta / R^3$, was empirically determined to be 2.6, where ω_0 is the natural frequency.
2. The damping in terms of the logarithmic decrement (δ) was experimentally determined to follow the relation $\delta = K_2 (\mu^2 / \rho \sigma R)^{1/4}$ where K_2 was empirically determined to be 21.6 and ρ and σ are liquid density and surface tension, respectively.
3. The logarithmic decrement was also expressed as $\delta = K'_1 (\mu / \rho \omega_0 R^2)^{1/2}$ permitting comparison with normal gravity results. K'_1 was determined to be 28.1, which is approximately four times greater than K_1 , the normal gravity constant.

Lewis Research Center,
National Aeronautics and Space Administration,
Cleveland, Ohio, April 4, 1967,
124-09-03-01-22.

REFERENCES

1. Reynolds, W. C.; Saad, M. A.; and Satterlee, H. M.: Capillary Hydrostatics and Hydrodynamics at Low G. Rep. No. LG-3, Stanford Univ., Sept. 1, 1964.
2. Yeh, Gordon C. K.; and Hutton, Robert E.: Fluid Mechanics at Low Gravity Environments. Rep. No. 9840-6005-RU-000, TRW Space Technology Lab., Dec. 1964.
3. Satterlee, H. M.; and Reynolds, W. C.: The Dynamics of the Free Liquid Surface in Cylindrical Containers under Strong Capillary and Weak Gravity Conditions. Rep. No. LG-2, Stanford Univ., May 1, 1964.
4. Koval, Leslie R.; and Bhuta, Pravin G.: A Direct Solution for Capillary-Gravity Waves in a Cylindrical Tank. Rep. No. 9840-6011-RU-000, TRW Space Technology Lab., Mar. 1965.
5. Lamb, Horace: Hydrodynamics. Sixth ed., Dover Publications, 1932 (Repr. 1945).
6. Case, K. M.; and Parkinson, W. C.: Damping of Surface Waves in an Incompressible Liquid. J. Fluid Mech., vol. 2, pt. 2, Mar. 1957, pp. 172-184.
7. Miles, John W.: On the Sloshing of Liquid in a Cylindrical Tank. Rep. No. AM 6-5, GM-TR-18, Ramo-Wooldridge Corp., Apr. 20, 1956.

8. Stephens, David G.; Leonard, H. Wayne; and Perry, Tom W., Jr.: Investigation of the Damping of Liquids in Right-Circular Cylindrical Tanks, Including the Effects of a Time-Variant Liquid Depth. NASA TN D-1367, 1962.
9. Sumner, Irving E.; and Stofan, Andrew J.: An Experimental Investigation of the Viscous Damping of Liquid Sloshing in Spherical Tanks. NASA TN D-1991, 1963.
10. Friz, G.: On the Dynamic Contact Angle in the Case of Complete Wetting. Z. A Angew. Phys., vol. 19, no. 4, July 1965, pp. 374-378.

"The aeronautical and space activities of the United States shall be conducted so as to contribute . . . to the expansion of human knowledge of phenomena in the atmosphere and space. The Administration shall provide for the widest practicable and appropriate dissemination of information concerning its activities and the results thereof."

—NATIONAL AERONAUTICS AND SPACE ACT OF 1958

NASA SCIENTIFIC AND TECHNICAL PUBLICATIONS

TECHNICAL REPORTS: Scientific and technical information considered important, complete, and a lasting contribution to existing knowledge.

TECHNICAL NOTES: Information less broad in scope but nevertheless of importance as a contribution to existing knowledge.

TECHNICAL MEMORANDUMS: Information receiving limited distribution because of preliminary data, security classification, or other reasons.

CONTRACTOR REPORTS: Scientific and technical information generated under a NASA contract or grant and considered an important contribution to existing knowledge.

TECHNICAL TRANSLATIONS: Information published in a foreign language considered to merit NASA distribution in English.

SPECIAL PUBLICATIONS: Information derived from or of value to NASA activities. Publications include conference proceedings, monographs, data compilations, handbooks, sourcebooks, and special bibliographies.

TECHNOLOGY UTILIZATION PUBLICATIONS: Information on technology used by NASA that may be of particular interest in commercial and other non-aerospace applications. Publications include Tech Briefs, Technology Utilization Reports and Notes, and Technology Surveys.

Details on the availability of these publications may be obtained from:

SCIENTIFIC AND TECHNICAL INFORMATION DIVISION

NATIONAL AERONAUTICS AND SPACE ADMINISTRATION

Washington, D.C. 20546